

## Ferrocene Encapsulated within Symmetric Dendrimers: A Deeper Understanding of Dendritic Effects on Redox Potential

Diane L. Stone,<sup>†</sup> David K. Smith,<sup>\*,†</sup> and P. Terry McGrail<sup>‡</sup>

Contribution from the Department of Chemistry, University of York, Heslington, York, YO10 5DD, U.K., and Cytecfiberite Ltd., Wilton Centre, Wilton, Redcar, TS10 4RF, U.K.

Received July 17, 2001

**Abstract:** Ferrocene has been encapsulated within a symmetric ether-amide dendritic shell and its redox potential monitored in a variety of solvents. The dendritic effect generated by the branched shell is different in different solvents. In less polar, non hydrogen bond donor solvents, attachment of the branched shell to ferrocene increases its  $E_{1/2}$ , indicating that oxidation to ferrocenium (charge buildup) becomes thermodynamically hindered by the dendrimer, a result explained by the dendrimer providing a less polar medium than that of the surrounding electrolyte solution. The effect of electrolyte concentration on redox potential was also investigated, and it was shown that the concentration of "innocent" electrolyte has a significant effect on the redox potential by increasing the overall polarity of the surrounding medium. Dendritic destabilization of charge buildup is in agreement with the majority of reported dendritic effects. A notable exception to this is provided by the asymmetric ferrocene dendrimers previously reported by Kaifer and co-workers, in which the branching facilitated oxidation, and it is proposed that in this case the dendritic effect is generated by a different mechanism. Interestingly, in methanol, the new symmetric ferrocene dendrimer exhibited almost no dendritic effect, a result explained by the ability of methanol to interact extensively with the branched shell, generating a more open superstructure. By comparison of all the new data with other reports, this study provides a key insight into the structure–activity relationships which control redox processes in dendrimers and also an insight into the electrochemical process itself.

### Introduction

The ability of a branched, dendritic<sup>1</sup> shell to generate a microenvironment,<sup>2</sup> modifying the properties of its functional core, is of intense current interest—primarily because it provides chemists with a method for generating new functional materials with modified properties, but also because it mimics the way in which a protein superstructure precisely controls the behavior of the active site.<sup>3</sup> Recently, much attention has focused on the way in which dendritic encapsulation of redox-active moieties alters their redox properties.<sup>4</sup> It is, for example, well established that dendritic encapsulation leads to a decrease in electrochemi-

cal reversibility, primarily as a consequence of the branched shell hindering electron transfer between the electrode surface and the buried redox-active subunit—analogue to the situation in redox-active proteins. The effect of dendritic structure on redox potential, however, has not been so easy to define. Diederich and co-workers have reported dendritic porphyrins which exhibit half-potentials shifted relative to their nondendritic analogues,<sup>5</sup> and the importance of these molecules for modeling the shifted redox potentials in biologically important proteins such as cytochromes has been discussed in some detail. In a similar vein, Mondal and Basu have very recently dendritically controlled the potential of a Mo<sup>VO</sup>S<sub>4</sub> core in order to model DMSO reductases.<sup>6</sup> In contrast, however, neither the dendritically modified porphyrins of Fréchet and co-workers<sup>7</sup> nor the numerous reported dendritically modified ruthenium(II) or iron(II) bipyridine and terpyridine complexes<sup>8</sup> show any shift in their redox potentials. The iron–sulfur clusters of Gorman and co-workers only exhibited dendritically modified redox potentials in thin films, not in DMF solution.<sup>9</sup> This contrast

\* To whom correspondence should be addressed. E-mail: dks3@york.ac.uk.

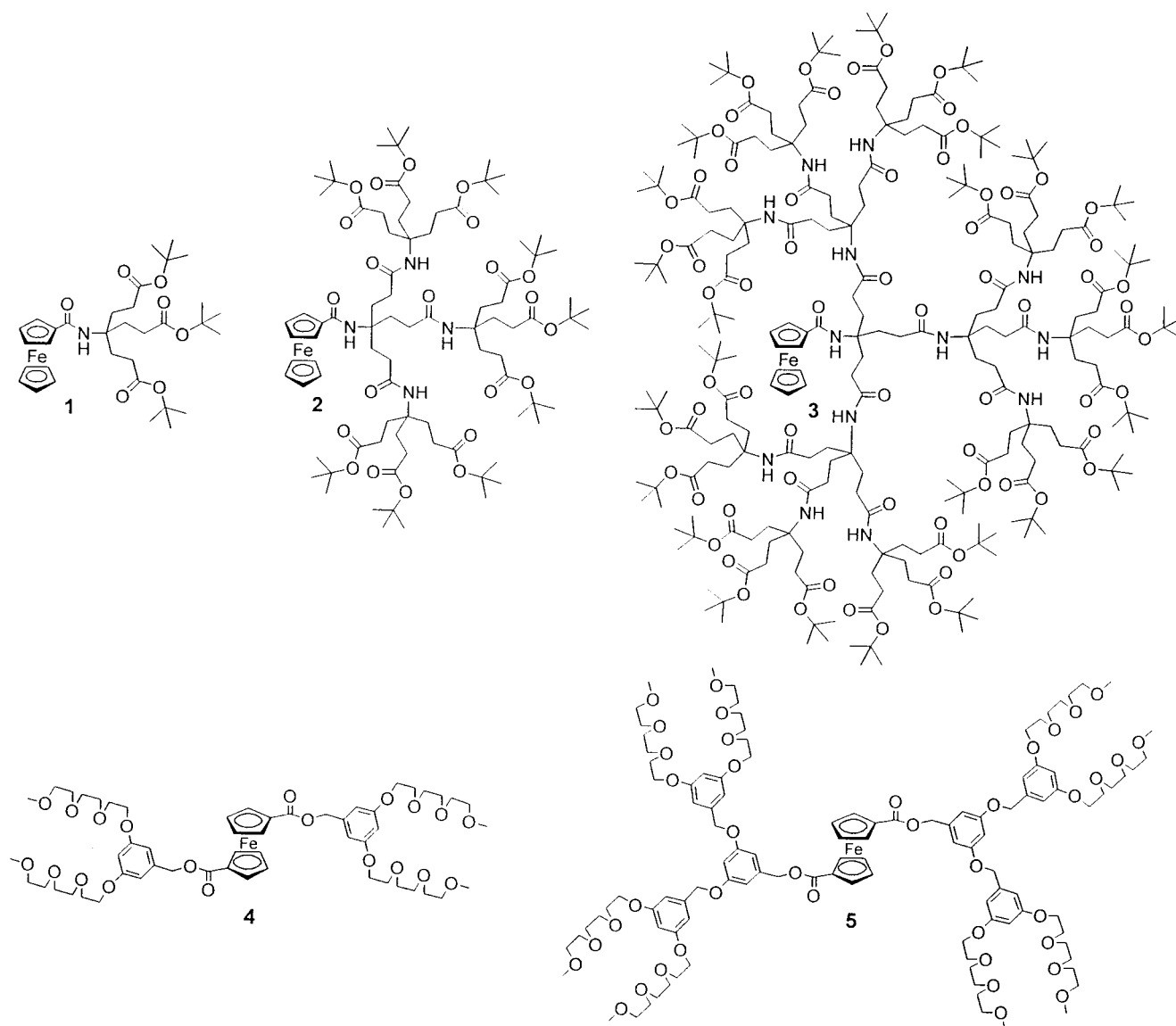
<sup>†</sup> University of York.

<sup>‡</sup> Cytecfiberite Ltd.

- (1) For general reviews of dendrimer chemistry, see: (a) Newkome, G. R.; Moorefield, C. N.; Vögtle, F. *Dendritic Molecules: Concepts, Syntheses, Perspectives*; VCH: Weinheim, 1996. (b) Chow, H.-F.; Mong, T. K.-K.; Nongrum, M. F.; Wan, C.-W. *Tetrahedron* **1998**, *54*, 8543. (c) Matthews, O. A.; Shipway, A. N.; Stoddart, J. F. *Prog. Polym. Sci.* **1998**, *23*, 1. (d) Fischer, M.; Vögtle, F. *Angew. Chem., Int. Ed.* **1999**, *38*, 884.
- (2) For the first report of a "dendritic microenvironment", see: Hawker, C. J.; Wooley, K. L.; Fréchet, J. M. J. *J. Am. Chem. Soc.* **1993**, *115*, 4375.
- (3) For a review conceptualizing the ability of dendrimers to act as functional models of biological systems, see: Smith, D. K.; Diederich, F. *Chem. Eur. J.* **1998**, *4*, 1353 and references therein.
- (4) For reviews concerning the effect of dendritic encapsulation on redox properties, see: (a) Gorman, C. B. *Adv. Mater.* **1998**, *10*, 295. (b) Bryce, M. R.; Devonport, W. *Adv. Dendritic Macromol.* **1996**, *3*, 115. (c) Gorman, C. B.; Smith, J. C. *Acc. Chem. Res.* **2001**, *34*, 60. (d) Hecht, S.; Fréchet, J. M. J. *Angew. Chem., Int. Ed.* **2001**, *40*, 74. (e) Cardona, C. M.; Mendoza, S.; Kaifer, A. E. *Chem. Soc. Rev.* **2000**, *29*, 37.

- (5) (a) Dandliker, P. J.; Diederich, F.; Gross, M.; Knobler, C. B.; Louati, A.; Sanford, E. M. *Angew. Chem., Int. Ed. Engl.* **1994**, *33*, 1739. (b) Dandliker, P. J.; Diederich, F.; Gisselbrecht, J.-P.; Louati, A.; Gross, M. *Angew. Chem., Int. Ed. Engl.* **1995**, *34*, 2725. (c) Dandliker, P. J.; Diederich, F.; Zingg, A.; Gisselbrecht, J.-P.; Gross, M.; Louati, A.; Sanford, E. *Helv. Chim. Acta* **1997**, *80*, 1773. (d) Weyermann, P.; Gisselbrecht, J.-P.; Boudon, C.; Diederich, F.; Gross, M. *Angew. Chem., Int. Ed.* **1999**, *38*, 3215.
- (6) Mondal, S.; Basu, P. *Inorg. Chem.* **2001**, *40*, 192.
- (7) Pollak, K. W.; Leon, J. W.; Fréchet, J. M. J.; Maskus, M.; Abruña, H. D. *Chem. Mater.* **1998**, *10*, 30.

Chart 1. Compounds 1–5



between results poses intriguing questions about the structure–activity relationships generated by dendritic branches with different structures.

To investigate structure–activity effects as unambiguously as possible, however, it is important to investigate the behavior of simple, well-behaved probe molecules. For example, our investigations of dendritically modified tryptophan derivatives have provided considerable insight into the modification of optical properties by individual hydrogen bond interactions from a dendritic branch.<sup>10</sup> Cardona and Kaifer have used ferrocene as a simple redox probe and published a series of ferrocenes

asymmetrically functionalized with dendritic branching constructed from aliphatic amide groups (1–3, Chart 1).<sup>11</sup> The presence of even relatively small quantities of dendritic branching markedly affected the metallocene redox potential, making oxidation to ferrocenium thermodynamically favored.

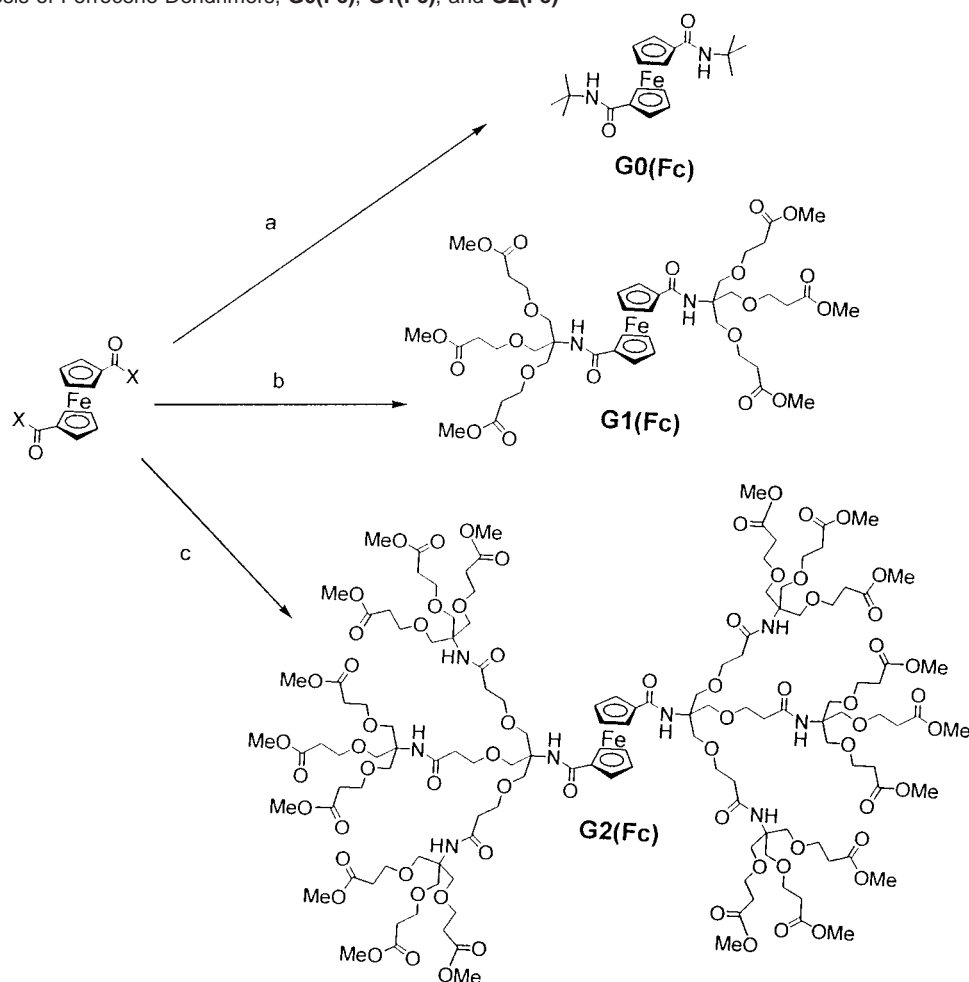
The relationship between dendritic structure and redox potential is a complex one. Dendritic structures can be more or less polar than the solvent and can interact in specific ways to alter redox potential. For these reasons, ferrocene is a particularly interesting and suitable redox-active probe of the dendritic environment due to its electrochemical simplicity, and we therefore decided to use it to investigate the dendritic effect on a series of symmetric dendritic ferrocene derivatives (4 and 5, Chart 1). We reported that small aromatic ether branches, unlike the aliphatic amide branches of Cardona and Kaifer, were unable to alter the redox potential, and we proposed that the rigidity of this dendritic system prevented it from having a major impact

(8) (a) Newkome, G. R.; Güther, R.; Moorefield, C. N.; Cardullo, F.; Echegoyen, L.; Pérez-Cordero, E.; Luftmann, H. *Angew. Chem., Int. Ed. Engl.* **1995**, *34*, 2023. (b) Chow, H.-F.; Chan, I. Y.-K.; Chan, D. T. W.; Kwok, R. W. M. *Chem. Eur. J.* **1996**, *2*, 1085. (c) Vögtle, F.; Plevoets, M.; Nieger, M.; Azzellini, G. C.; Credi, A.; De Cola, L.; De Marchis, V.; Venturi, M.; Balzani, V. *J. Am. Chem. Soc.* **1999**, *121*, 6290. (d) Chow, H. F.; Chan, I. Y. K.; Fung, P. S.; Mong, T. K. K.; Nongrum, M. F. *Tetrahedron* **2001**, *57*, 1565.

(9) (a) Gorman, C. B. *Adv. Mater.* **1997**, *9*, 1117. (b) Gorman, C. B.; Parkhurst, B. L.; Su, W. Y.; Chen, K. Y. *J. Am. Chem. Soc.* **1997**, *119*, 1141. (c) Gorman, C. B.; Smith, J. C. *J. Am. Chem. Soc.* **2000**, *122*, 9342.

(10) (a) Smith, D. K.; Müller, L. *Chem. Commun.* **1999**, 1915. (b) Koenig, S.; Müller, L.; Smith, D. K. *Chem. Eur. J.* **2001**, *7*, 979.

(11) (a) Cardona, C. M.; Kaifer, A. E. *J. Am. Chem. Soc.* **1998**, *120*, 4023. (b) Wang, Y.; Cardona, C. M.; Kaifer, A. E. *J. Am. Chem. Soc.* **1999**, *121*, 9756. (c) Cardona, C. M.; McCarley, T. D.; Kaifer, A. E. *J. Org. Chem.* **2000**, *65*, 1857.

**Scheme 1.** Synthesis of Ferrocene Dendrimers, **G0(Fc)**, **G1(Fc)**, and **G2(Fc)**<sup>a</sup>

<sup>a</sup> Conditions: (a) (X = F) *tert*-butylamine, DMAP, CH<sub>2</sub>Cl<sub>2</sub>, 74%; (b) (X = Cl) dendritic branch **6**, DMAP, CH<sub>2</sub>Cl<sub>2</sub>, 51%; (c) (X = F) dendritic branch **7**, DMAP, CH<sub>2</sub>Cl<sub>2</sub>, 34%.

on the redox potential of the encapsulated core.<sup>12</sup> Indeed, the majority of systems reported in which the dendritic shell has little effect on redox potential use relatively rigid branches. In such systems, the only dendritic effect is a decrease in electrochemical reversibility. This paper extends our research and reports a new series of dendrimers in which flexible dendritic branches are attached to a ferrocene core in a symmetric manner. We have investigated their electrochemical properties in a range of different solvents and have found marked dendritic effects on redox potential, but only in certain solvents. Remarkably, the shift in redox potential is opposite to that reported by Cardona and Kaifer, and this enables us to draw some general conclusions about the way in which a branched shell can control encapsulated functional groups. In this paper we report on the new insights that this gives us into structure–activity relationships in dendrimers, and also the information this gives us about the nature of electrochemical processes in general.

## Results and Discussion

### Synthesis and Characterization of Ferrocene Dendrimers.

Target molecules **G0(Fc)**, **G1(Fc)**, and **G2(Fc)** were synthesized via a convergent coupling strategy as shown in Scheme 1, in

which either 1,1'-bis(chlorocarbonyl)ferrocene<sup>13</sup> or 1,1'-bis-(fluorocarbonyl)ferrocene<sup>14</sup> was coupled with <sup>t</sup>BuNH<sub>2</sub> or pre-formed dendritic branches of first (**6**) or second (**7**) generation, respectively (Chart 2). These dendritic branches were synthesized according to the methodology previously reported by Newkome and co-workers and subsequently modified by Diederich and co-workers.<sup>15</sup> Coupling of the branches to the redox-active ferrocene subunit was achieved using DMAP or NEt<sub>3</sub> as base. It was notable that as the bulk of the dendritic branches increased, the yield of the desired product dropped.

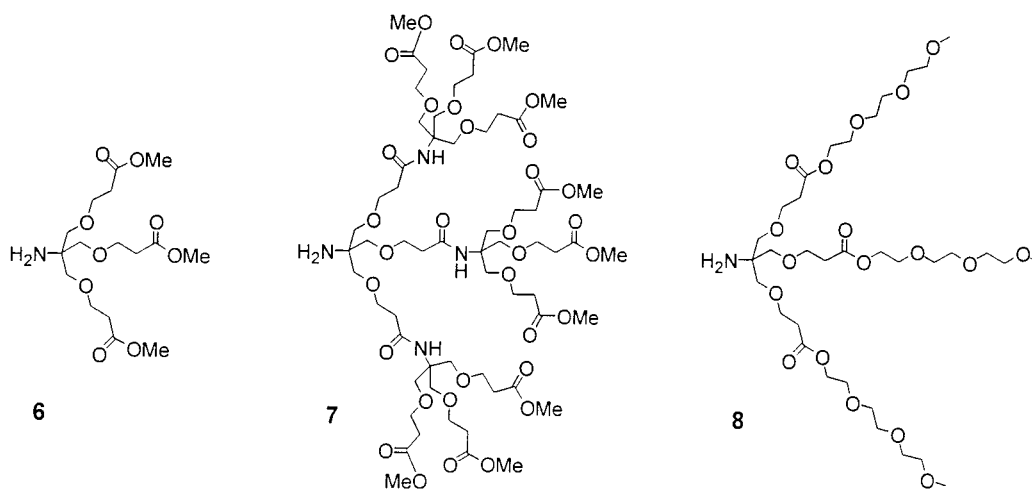
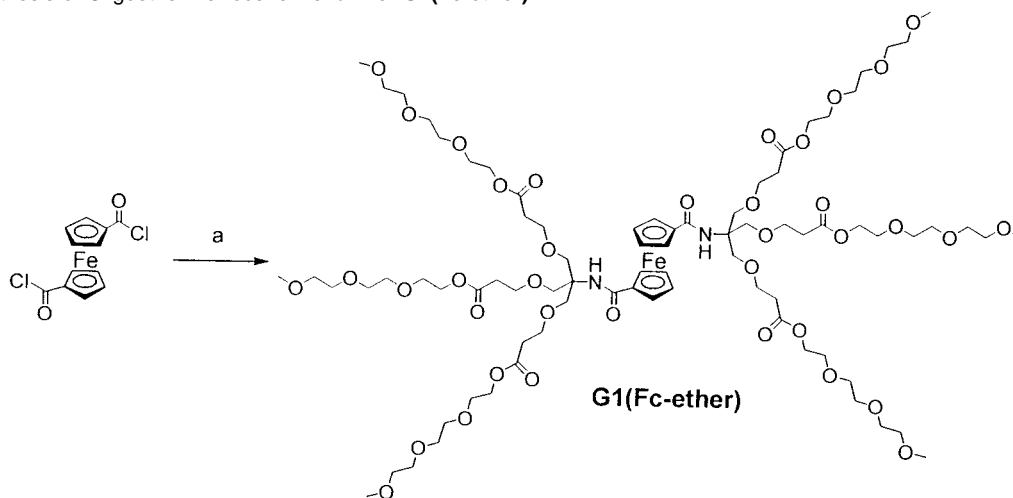
This effect is expected in convergent dendrimer syntheses as the reactive group at the focal point of the dendritic branch becomes increasingly sterically crowded as the dendritic generation increases. It is interesting to note that the reaction with second generation dendritic branches represents the limit for effective coupling between this core and dendritic branches and could only be achieved in relatively low yield. This agrees with our previous investigations using the less highly branched

(13) Lorkowski, H. J.; Pannier, R.; Wende, A. *J. Prakt. Chem.* **1967**, *35*, 149.  
(14) Galow, T. H.; Rodrigo, J.; Cleary, K.; Cooke, G.; Rotello, V. M. *J. Org. Chem.* **1999**, *64*, 3745.

(15) (a) Newkome, G. R.; Lin, X. *Macromolecules* **1991**, *24*, 1443. (b) Newkome, G. R.; Lin, X.; Weis, C. D. *Tetrahedron: Asymmetry* **1991**, *2*, 957. (c) Young, J. K.; Baker, G. R.; Newkome, G. R.; Morris, K. F.; Johnson, C. S., Jr. *Macromolecules* **1994**, *27*, 3464. (d) Nierengarten, J.-F.; Habicher, T.; Kessinger, R.; Cardullo, F.; Diederich, F.; Gramlich, V.; Gisselbrecht, J.-P.; Boudon, C.; Gross, M. *Helv. Chim. Acta* **1997**, *80*, 2238.

(12) Smith, D. K. *J. Chem. Soc., Perkin Trans. 2* **1999**, 1563.

Chart 2. Dendritic Branches 6–8

Scheme 2. Synthesis of Oligoether Ferrocene Dendrimer **G1(Fc-ether)**<sup>a</sup>

<sup>a</sup> Conditions: dendritic branch **8**, DMAP, THF, 73%.

aromatic ether cascade in which the bis-substituted second generation dendrimer (**5**) could be synthesized, while third generation branches would only couple once onto the ferrocene core.<sup>12</sup> This gives an indication of the relative size constraints of the different types of dendritic branching—the 3-fold ether-amide cascade is more sterically demanding than that constructed from 2-fold branched aromatic ethers.

The novel dendrimers were characterized using a range of techniques—<sup>1</sup>H NMR, <sup>13</sup>C NMR, electrospray mass spectrometry, infrared spectrometry, and gel permeation chromatography—as well as cyclic voltammetry (details below). All characterization data were consistent with the nature of these products. There are, however, some notable points from the characterization of **G2(Fc)**. The <sup>1</sup>H NMR (and <sup>13</sup>C NMR) spectrum was in agreement with the proposed product, although the Fc-H protons were significantly broadened—consistent with the steric constraints of the dendritic branches hindering free rotation of the Cp rings. Gel permeation chromatography clearly indicated that the reaction gave rise to three products—unfunctionalized, mono-functionalized, and bis-functionalized cores. These products were separated on a preparative gel column (Biobeads SX-1), and the band corresponding to bis-functionalized product was collected. Analytical GPC (Shodex columns, eluent THF) confirmed this product as monodisperse. A GPC calibration was

applied (using linear polystyrene standards), and the mass of **G2(Fc)** was calculated as 2606 ( $M_r = 3078$ ). Although the calculated mass was somewhat below the theoretical value, this was not unexpected as polystyrene standards are linear polymers, while the product is spherical (with GPC retention times being dependent on exclusion volume, not molecular mass), and the agreement was therefore considered reasonable. In the mass spectrum (electrospray), the base peak corresponded to a doubly charged ion  $[M + 2Na]^{2+}$ , although a fragment peak was also observed in which a dendritic branch connected to a Cp ring had been removed from the molecule. All other characterization (IR, CV) was fully consistent with the proposed structure.

A further target dendrimer, **G1(Fc-ether)**, in which the dendritic periphery is functionalized by oligoether chains, was synthesized by convergently coupling first generation oligoether substituted branches (**8**, Chart 2) with 1,1'-bis(chlorocarbonyl)ferrocene (Scheme 2). Attempts were made to synthesize the second generation analogue of this molecule using a convergent strategy, but the coupling reaction was unsuccessful, with no trace of product being observed by gel permeation chromatography—presumably as a consequence of the even greater steric hindrance of the single reactive amine group at the focal point of the dendritic branch. This once again indicates the steric limitations of the convergent approach to synthesis

**Table 1.** Redox Potentials ( $E_{1/2} = (E_{ox} - E_{red})/2$ ) of Ferrocene (Fc) and Dendrimers **G0(Fc)**, **G1(Fc)**, **G2(Fc)**, and **G1(Fc-ether)** in Different Solvents

solvent	Fc	G0(Fc)	G1(Fc)	G2(Fc)	G1(Fc-ether)
THF	0.641 <sup>b</sup>	0.897 <sup>b</sup>	0.927 <sup>b</sup>		
CHCl <sub>3</sub>	0.606 <sup>b</sup>	0.871 <sup>b</sup>	0.942 <sup>b</sup>		0.942 <sup>b</sup>
CH <sub>2</sub> Cl <sub>2</sub>	0.583 <sup>b</sup>	0.875 <sup>b</sup>	0.914 <sup>b</sup>	0.953 <sup>b</sup>	0.885 <sup>a</sup>
CH <sub>3</sub> CN	0.490 <sup>a</sup>	0.786 <sup>a</sup>	0.818 <sup>a</sup>	0.929 <sup>a</sup>	0.807 <sup>a</sup>
	0.483 <sup>b</sup>				
EtOH	0.484 <sup>a</sup>	0.801 <sup>b</sup>	0.830 <sup>a</sup>		0.814 <sup>b</sup>
	0.481 <sup>b</sup>				
MeOH	0.439 <sup>a</sup>	0.790 <sup>a</sup>	0.797 <sup>a</sup>	0.801 <sup>a</sup>	0.795 <sup>a</sup>
	0.433 <sup>b</sup>				

<sup>a</sup> [Bu<sub>4</sub>N<sup>+</sup>][BF<sub>4</sub><sup>-</sup>] = 0.2 M. <sup>b</sup> [Bu<sub>4</sub>N<sup>+</sup>][BF<sub>4</sub><sup>-</sup>] = 0.5 M. Redox potentials are quoted in volts relative to Ag/Ag<sup>+</sup> reference and measured at a scan rate of 200 mV s<sup>-1</sup>. All potentials are ±5 mV.

in this case. Attempts were also made to synthesize these dendrimers using the divergent approach, but these were unsuccessful as a consequence of the fragility of the ferrocene core and the difficulty of isolating some of the highly polar intermediates.

**Electrochemical Investigations.** The dendrimers synthesized were investigated using cyclic voltammetry in a range of different solvents (Table 1), as was ferrocene itself.<sup>16</sup> In some cases, where reversibility was lower, square wave voltammetry was also used to confirm the  $E_{1/2}$  values. The solvents were chosen to span the range from nonpolar to polar and from non-hydrogen-bonding to hydrogen-bonding. Dendrimer **G2(Fc)** was only investigated in three representative solvents (due to lack of material).

As expected, the functionalized ferrocenes were harder to oxidize than ferrocene itself, as a consequence of the electron-withdrawing effect of the amide groups. Interestingly, all compounds investigated exhibited different redox potentials in different solvents. In particular, oxidation becomes less favored in less polar solvents. This result was expected on the basis of more polar media being better able to stabilize the oxidized ferrocenium cation—it is indeed well-known that the redox potential of unfunctionalized ferrocene varies in such a manner with solvent polarity.<sup>17</sup>

The focus of this study, however, was placed on understanding the way in which attaching dendritic branching affected the redox behavior. As has been reported in many other studies of dendritically encapsulated redox centers, the reversibility of the redox couple decreased as the extent of dendritic branching increased, although even for **G2(Fc)** a clear reversible CV wave was still obtained. Particularly interesting in this case, however, was the effect of branching on the redox potential. The redox potentials of **G0(Fc)**, **G1(Fc)**, and **G2(Fc)** are represented graphically in Figure 1. It is immediately obvious that the attachment of dendritic branches to the core has a dramatic effect on the observed redox potential, particularly in CH<sub>2</sub>Cl<sub>2</sub> and CH<sub>3</sub>CN solution. This effect is already clear when comparing **G0(Fc)** with **G1(Fc)**. The trend toward increasing difficulty of oxidation caused by dendritic functionalization is then continued, with **G2(Fc)** being more difficult to oxidize than **G1(Fc)**. **G0(Fc)** was chosen as a model system because it mimics the

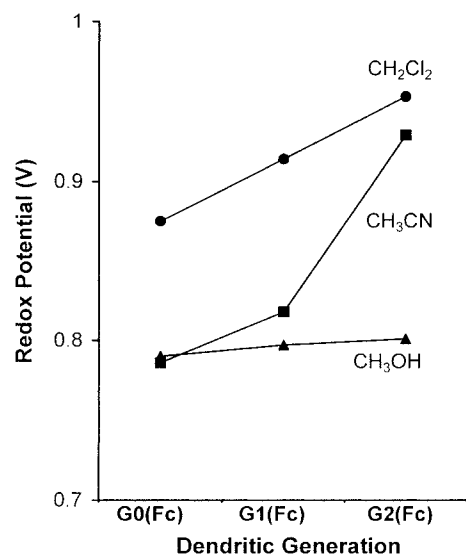


**Figure 1.** Effect of dendritic generation on redox potential ( $E_{1/2}$ ) of symmetric ferrocene dendrimers **G0(Fc)**, **G1(Fc)**, and **G2(Fc)** in CH<sub>2</sub>Cl<sub>2</sub> (0.5 M, [Bu<sub>4</sub>N<sup>+</sup>][BF<sub>4</sub><sup>-</sup>]), CH<sub>3</sub>CN (0.2 M, [Bu<sub>4</sub>N<sup>+</sup>][BF<sub>4</sub><sup>-</sup>]), and MeOH (0.2 M, [Bu<sub>4</sub>N<sup>+</sup>][BF<sub>4</sub><sup>-</sup>]).

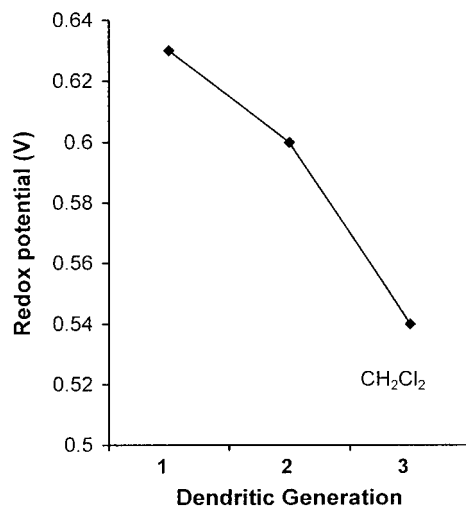


**Figure 2.** Effect of dendritic generation on redox potential ( $E_{1/2}$ ) of asymmetric ferrocene dendrimers **3–5** in CH<sub>2</sub>Cl<sub>2</sub> (0.2 M, [Bu<sub>4</sub>N<sup>+</sup>][PF<sub>6</sub><sup>-</sup>]).

local environment of the ferrocene core, in particular the “through-bond” effects on redox potential which will be exerted by the branched amide substituents.

This result is in marked contrast with our previous report of symmetrical dendrimers **4** and **5** in which the relatively rigid branching caused no shift of the redox potential.<sup>12</sup> Our observation of a dendritic effect for **G0(Fc)**, **G1(Fc)**, and **G2(Fc)** would therefore confirm our previous conclusion that branch flexibility plays a key role in allowing efficient encapsulation and property modification of functional cores.

Interestingly, however, the results reported here are also in sharp contrast with those reported by Cardona and Kaifer for their series of asymmetric ferrocene dendrimers (**1**, **2**, and **3**), functionalized with a similar type of flexible dendritic branching.<sup>11</sup> For dendrimers **1**, **2**, and **3**, the attachment of dendritic branching led to a reduction in the redox potential, indicating that ferrocene oxidation becomes thermodynamically favored (Figure 2). For dendrimers **G0(Fc)**, **G1(Fc)**, and **G2(Fc)**, however, the redox potential increases with increasing dendritic

(16) Cyclic voltammetry performed at 25 °C with tetra-*n*-butylammonium tetrafluoroborate as background electrolyte. Platinum electrode as working, platinum wire as counter, and Ag/Ag<sup>+</sup> (in H<sub>2</sub>O) as reference. All redox potentials are quoted referenced to Ag/Ag<sup>+</sup>.

(17) Noviandri, I.; Brown, K. N.; Fleming, D. S.; Gulyas, P. T.; Lay, P. A.; Masters, A. F.; Phillips, L. *J. Phys. Chem. B* **1999**, *103*, 6713.

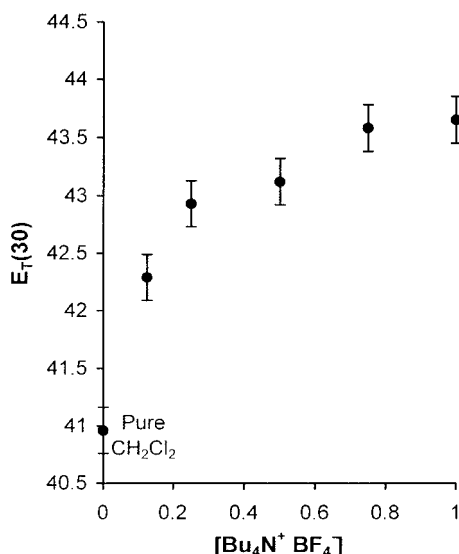


**Figure 3.** Correlation between the concentration of base electrolyte in CH<sub>2</sub>Cl<sub>2</sub> and the solvent  $E_T(30)$  value as calculated using Reichardt's dye, indicating that the more concentrated the solution, the greater its polarity.

generation, indicating that the branching thermodynamically hinders ferrocene oxidation.

This dramatic difference must be a consequence of the different structures of the two series of molecules. There are some minor structural difference between the two series of dendrimers: i.e., the presence or absence of ether linkages, and methyl or *tert*-butyl esters at the periphery. It is difficult to see, however, how these changes could induce a complete reversal of the dendritic effect. The most significant difference between the two series of dendrimers is symmetry. Dendrimers 1–3 are asymmetric, while **G0(Fc)**, **G1(Fc)**, and **G2(Fc)** are fully symmetric structures. A greater degree of core encapsulation might be expected for the symmetric series of dendrimers. We therefore propose that for **G2(Fc)** the dendritic branching hinders oxidation by providing a microenvironment<sup>2,3</sup> for ferrocene that is less polar/ionic than the surrounding electrolyte solution. In analogy, it is often stated that the interiors of proteins are relatively nonpolar, although this low polarity is in comparison to their surrounding aqueous environment. It may seem surprising that for **G1(Fc)** and **G2(Fc)**, the dendritic branches, which contain multiple amide and ether groups analogous to proteins, create a microenvironment that is *even less polar* than the nonpolar solvents in which they are dissolved: CHCl<sub>3</sub> ( $\epsilon = 4.8$ ), THF ( $\epsilon = 7.6$ ), or CH<sub>2</sub>Cl<sub>2</sub> ( $\epsilon = 8.9$ ). It must be remembered, however, that electrochemical investigations are not performed in neat organic solvents, but in ionic solutions of electrolyte (in this case typically 0.2 M tetrabutylammonium tetrafluoroborate), the presence of which would be expected to increase the solvent polarity.

We therefore experimentally determined the effect of electrolyte on the polarity of CH<sub>2</sub>Cl<sub>2</sub> using the UV–vis absorption wavelength of Reichardt's dye in electrolyte solutions of different concentrations to generate  $E_T(30)$  values.<sup>18</sup> The relationship between [electrolyte] and solvent polarity is illustrated in Figure 3. In fact, a 0.2 M solution of tetrabutylammonium tetrafluoroborate in CH<sub>2</sub>Cl<sub>2</sub> has a polarity equivalent

**Table 2.** Redox potentials ( $E_{1/2} = (E_{ox} - E_{red})/2$ ) of Ferrocene and Dendrimer **G1(Fc)** in CH<sub>2</sub>Cl<sub>2</sub> Containing Different Amounts of Base Electrolyte (Bu<sub>4</sub>N<sup>+</sup>BF<sub>4</sub><sup>-</sup>)<sup>a</sup>

[base electrolyte] (M)	$E_T(30)$	$E_{1/2}$ (V)	
		Fc	G1(Fc)
0.125	42.29	0.626	0.931
0.25	42.93	0.605	0.925
0.5	43.12	0.583	0.914
0.75	43.58	0.574	0.904
1.0	43.65	0.566	0.898

<sup>a</sup> Redox potentials are quoted in volts relative to Ag/Ag<sup>+</sup> reference and measured at a scan rate of 200 mV s<sup>-1</sup>. All potentials are  $\pm 5$  mV.  $E_T(30)$  values were calculated from the absorption wavelength of a solution of Reichardt's dye in the given solvent.<sup>18</sup>

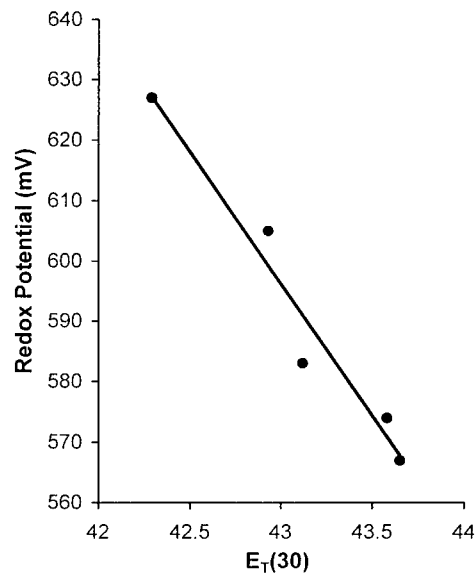


**Figure 4.** Correlation between the  $E_T(30)$  value of CH<sub>2</sub>Cl<sub>2</sub> containing different concentrations of base electrolyte and the redox potential of ferrocene (versus Ag/Ag<sup>+</sup>).

to that of butanenitrile. In addition to simply increasing the polarity, the electrolyte can take part in ion–ion interactions with the oxidized ferrocenium species—stabilizing it. Such ion-pairing interactions, even using bulky ions such as Bu<sub>4</sub>N<sup>+</sup> or BF<sub>4</sub><sup>-</sup>, are well known and have been shown to play an important role in supramolecular chemistry in apolar solvents.<sup>19</sup> Ion pairing between electrolyte and Fc<sup>+</sup> will be limited by the presence of the bulky dendritic shield in **G1(Fc)** and **G2(Fc)**, hence hindering the oxidation process.

To investigate whether the branching does indeed act as a nonpolar shield, protecting the redox-active core from the polar, ionic electrolyte solution, we studied the effect of [electrolyte] on redox potential. The redox potential of ferrocene in CH<sub>2</sub>Cl<sub>2</sub> is strongly dependent on the concentration of electrolyte in which it is measured (Table 2). In fact, as might be expected, the redox potential of ferrocene could be correlated with the  $E_T(30)$  value of the electrolyte solution (as calculated above) (Figure 4).

We also measured the dependence of the redox potential of **G1(Fc)** on the concentration of electrolyte in CH<sub>2</sub>Cl<sub>2</sub> and found a similar but lesser dependence on [electrolyte]. The ability of electrolyte to alter redox potential in this way has been discussed

(18) Reichardt, C. *Solvents and Solvent Effects in Organic Chemistry*, 2nd ed.; VCH: Weinheim, 1990.

(19) (a) Beer, P. D.; Graydon, A. R.; Johnson, A. O. M.; Smith, D. K. *Inorg. Chem.* **1997**, *36*, 2112. (b) Pochapsky, S. S.; Mo, H.; Pochapsky, T. C.; *J. Chem. Soc., Chem. Commun.* **1995**, 2513.

previously;<sup>20</sup> however, our results shed an interesting light on factors which must be considered when using ferrocene as a reference in electrochemical studies.<sup>21</sup> It should also be noted that the role of electrolyte cannot be ignored when performing correlations of electrochemical behavior with solvent parameters—a factor often ignored in the literature.

To probe the polarity of the dendrimers further, we monitored the effect of the dendrimers themselves on the  $E_T(30)$  value of  $\text{CH}_2\text{Cl}_2$  using Reichardt's dye. At the concentration of the electrochemical experiment, neither **G0(Fc)** nor **G1(Fc)** had any impact on the apparent polarity of the solvent as measured by the  $\lambda_{\text{max}}$  of Reichardt's dye. This emphasizes that the effect of the dendritic shell on the redox potential of the ferrocene core is a *local effect experienced only within the dendritic interior* and is not caused by generalized bulk solvent polarity effects.

We therefore suggest that for **G0(Fc)**, **G1(Fc)**, and **G2(Fc)**, the dendritic branches operate by shielding the core from the relatively polar, ionic electrolyte solution, preventing ion–ion interactions, and thus hindering the generation of a charged species (i.e., oxidation). A closer examination of the literature, in fact, indicates that in the majority of cases where a dendritic redox shift has been reported<sup>4–7</sup> (other than that of Cardona and Kaifer,<sup>11a</sup> and one report from Diederich and co-workers<sup>5a</sup>), the dendritic branching hinders the buildup of charge (either positive or negative). It is also worthy of note that electrochemical experiments are unique among the experiments designed to probe dendritic effects in that they are carried out in electrolyte solutions, *not* pure solvents.

Why, then, do the dendrimers of Cardona and Kaifer have dendritic branching that appears to encourage the buildup of charge? We propose that the asymmetric nature of dendrimers **1–3** leads to less complete encapsulation. Indeed, Kaifer and co-workers have reported that related dendrimers are capable of orienting themselves at electrode surfaces in order to achieve facile electron transfer between the electrode and the proximate ferrocene unit—indicating the incomplete encapsulation of the redox-active unit in this case.<sup>11b</sup> We therefore speculate that the observed shift in potential in this case is generated by another mechanism. The dendritic effect could, for example, be caused by hydrogen bond interactions between the dendritic shell and ferrocene itself (electron pair donors in the shell will stabilize  $\text{Fc}^+$  and facilitate oxidation).<sup>22</sup> Although this is a speculative suggestion, it is, nonetheless, well known in the literature that hydrogen bond interactions can alter the redox potential of ferrocenes<sup>17</sup> and, in addition, play important roles in modifying the redox properties of biological systems.<sup>23</sup> There have also been a number of reports of dendrimers in which hydrogen-bonding interactions between branch and core have been shown to be important in controlling the behavior of the encapsulated unit.<sup>10,24</sup>

(20) McDevitt, M. R.; Addison, A. W. *Inorg. Chim. Acta* **1993**, *204*, 141.

(21) Although ferrocene is often used as an internal standard, and it may be considered that this negates solvent and base electrolyte mediated effects, it is noteworthy that, in this case, ferrocene was affected much more strongly than the functionalized systems **G0(Fc)**, **G1(Fc)**, and **G2(Fc)**. The use of ferrocene as a reference in this case can therefore be misleading, particularly when comparing the behavior of the dendrimers in different solvents, as the solvent effects on the redox potential of ferrocene significantly outweigh those on the redox potential of the species of interest.

(22) Such factors could also play a role in the redox modification of the symmetric ferrocene dendrimers, but it is likely that the encapsulation from electrolyte solution is the dominant factor for these molecules.

(23) See, for example: (a) Low, D. W.; Hill, M. G. *J. Am. Chem. Soc.* **2000**, *122*, 11039. (b) Sivakolundu, S. G.; Mabrouk, P. A. *J. Am. Chem. Soc.* **2000**, *122*, 1513.

These results with different types of ferrocene dendrimers are of considerable interest in terms of biomimicry. The proposal that dendritic effects on redox potential can occur through several different mechanisms has a direct parallel in the behavior of redox-active proteins. It is well established that the potentials of redox-active units in proteins are controlled by both the folding of the protein (which creates a nonpolar shielded environment) and the existence of specific ligation interactions at the metal ion.<sup>25</sup> The nonpolar shielded environment generated by the branched shell of our symmetric dendrimers is analogous to the superstructure of a protein, which has limited polarizability.<sup>26</sup> The results obtained with these dendritic model systems are therefore in agreement with such different factors also playing a leading role in controlling the redox properties of dendrimers.

Our results, however, also have some other very interesting features. In methanol, the dendritic branching appears to have little effect on the redox potential. This was initially surprising, as it was expected that the branching should shield the redox-active core from this polar solvent. However, MeOH can form multiple hydrogen bond interactions with the dendritic shell and, as a consequence of this and its small size, will solvate the structure very effectively. We therefore argue that the dendritic structure is solvated or “open” to a greater extent than in apolar solvents such as  $\text{CH}_2\text{Cl}_2$ . This would reduce the ability of the branching to shield the redox-active core from solvent and electrolyte and hence reduce the dendritic effect.

Solvent-controlled encapsulation processes, with “good” solvents opening up the superstructure, have recently been reported by several other groups.<sup>27</sup> Controlling the topology of the dendritic superstructure via solvation provides a simple way of switching dendritic encapsulation on and off, and a number of potential applications of this technology to property control and guest binding processes are currently under further investigation in this laboratory.

Many dendrimers reported in the literature utilize an oligoether periphery to achieve a good solubility profile in polar solvents, including water.<sup>5,24,28</sup> To investigate the effect of an oligoether dendritic periphery on the electrochemical process in this case, dendrimer **G1(Fc-ether)** was also studied by cyclic voltammetry. Interestingly, this compound showed a significant decrease in reversibility (Figure 5), the cyclic voltammogram being even less reversible than that for **G2(Fc)** in all solvents. In fact, it was only possible to generate approximate  $E_{1/2}$  values using square wave voltammetry. This is an interesting result because many previously reported oligoether-substituted den-

(24) (a) Collman, J. P.; Fu, L.; Zingg, A.; Diederich, F. *Chem. Commun.* **1997**, 193. (b) Smith, D. K.; Diederich, F. *Chem. Commun.* **1998**, 2501. (c) Smith, D. K.; Zingg, A.; Diederich, F. *Helv. Chim. Acta* **1999**, *82*, 1225.

(25) (a) Tezcan, F. A.; Winkler, J. R.; Gray, H. B. *J. Am. Chem. Soc.* **1998**, *120*, 13383. (b) Malmström, B. G.; Wittung-Stafshede, P. *Coord. Chem. Rev.* **1999**, *186*, 127. (c) Gunner, M. R.; Alexov, E.; Torres, E.; Lipovaca, S. *J. Biol. Inorg. Chem.* **1997**, *2*, 126.

(26) For an excellent overview of the electrostatic environment inside proteins, see: Warshel, A.; Papazyan, A. *Curr. Opin. Struct. Biol.* **1998**, *8*, 211.

(27) (a) Vinogradov, S. A.; Lo, L.-W.; Wilson, D. F. *Chem. Eur. J.* **1999**, *5*, 1338. (b) Hecht, S.; Vladimirov, N.; Fréchet, J. M. J. *J. Am. Chem. Soc.* **2001**, *123*, 18. (c) Pan, Y.; Ford, W. T. *Macromolecules* **2000**, *33*, 3731. (d) Topp, A.; Bauer, B. J.; Tomalia, D. A.; Amis, E. J. *Macromolecules* **1999**, *32*, 7232. (e) Backer, S.; Prinzie, Y.; Verheijen, W.; Smet, M.; Desmedt, K.; Dehaen, W.; De Schryver, F. C. *J. Phys. Chem. A* **1998**, *102*, 5451.

(28) (a) Mattei, S.; Seiler, P.; Diederich, F.; Gramlich, V. *Helv. Chim. Acta*, **1995**, *78*, 1904. (b) Mattei, S.; Wallimann, P.; Seiler, P.; Diederich, F. *Helv. Chim. Acta* **1997**, *80*, 2391. (c) Habicher, T.; Diederich, F.; Gramlich, V. *Helv. Chim. Acta* **1999**, *82*, 1066.

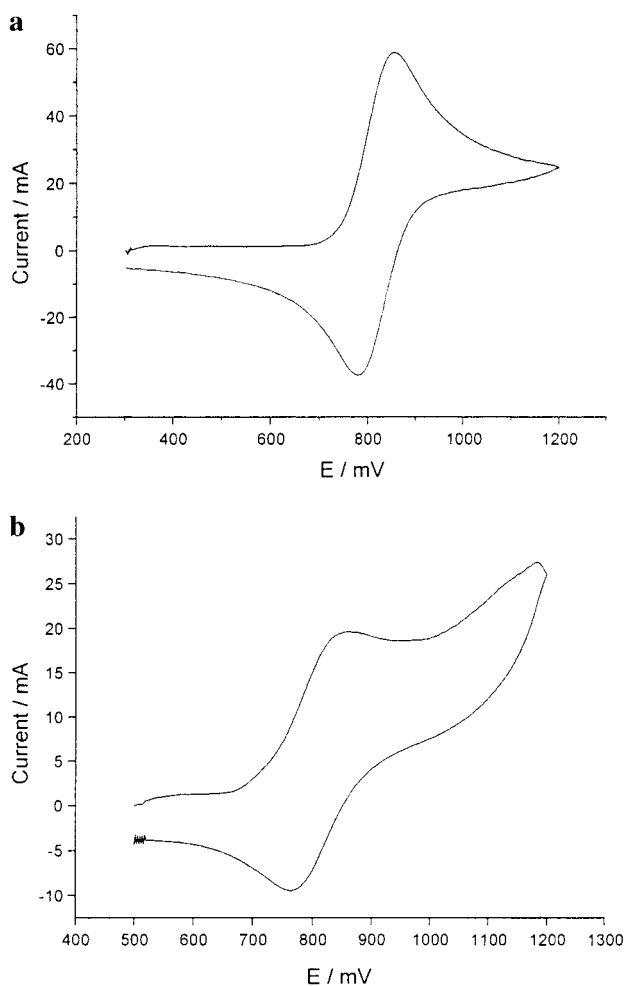


**Figure 5.** Cyclic voltammograms of **G1(Fc)** (a) and **G1(Fc-ether)** (b) (both 1 mM) illustrating the decrease in reversibility generated by the addition of polyether surface groups. Solvent  $\text{CH}_3\text{CN}$ , [base electrolyte] = 0.2 M, scan rate =  $200 \text{ mV s}^{-1}$ .

drimers show very low redox reversibility—an observation which can now be directly correlated to the presence of this modified dendritic surface.<sup>5</sup> This is possibly a consequence of increased encapsulation of the redox-active core (although some electrode adsorption was also observed on repeat scanning). Enhanced encapsulation using oligoether-functionalized dendritic branches has been previously reported.<sup>28c</sup> Comparison of the redox potentials of **G1(Fc)** and **G1(Fc-ether)** in different solvents, however, indicated that the attachment of an oligoether periphery generally had only minor effects on the  $E_{1/2}$  value.

## Conclusions and Outlook

These experiments show the ability of simple dendritic model systems to shed light on the nature of dendritic encapsulation. In particular, the attachment of a symmetric flexible branched shell has a significant impact on the redox potential of an encapsulated ferrocene derivative, with the buildup of charge (i.e., oxidation) being thermodynamically hindered by the presence of the branching. This observation is in agreement with the majority of other observations of dendritic effects on redox potential, with a noteworthy exception being the asymmetric dendritic ferrocenes (**1–3**). It is proposed that in the symmetric dendrimers, the branched shell acts as a nonpolar shield, analogous to a protein superstructure, protecting the redox-active

unit from the polar ionic electrolyte solution, thus destabilizing the charged form of the dendritic core. In the asymmetric ferrocene dendrimers, however, the polar electrolyte solution can still approach the less completely encapsulated redox-active subunit. It is suggested that the dendritic effect observed previously for asymmetric ferrocenyl dendrimers could operate through another mechanism, possibly hydrogen-bonding interactions. Furthermore, we report that the redox potential of symmetric ferrocene dendrimers (and hence the encapsulation) is controlled by the solvent. The dendritic branching exerts little shielding effect in the “good” solvent, methanol, possibly due to more effective solvation of the branched shell. In addition to providing further information about the true nature of the dendritic effect in electrochemistry, these results emphasize the important role played by electrolyte in electrochemical experiments, especially in nonpolar organic solvents. Furthermore, they indicate the ability of dendritic molecules to mimic the function and behavior of biological systems.

## Experimental Section

All  $^1\text{H}$  and  $^{13}\text{C}$  NMR studies were carried out on either a JEOL-E270 (270 MHz) or a Bruker AMX 500 (500 MHz) instrument, according to requirements and referenced to residual solvent. Neat IR studies, carried out on oil-like compounds, were measured on a Mattson Genesis Series FTIR spectrometer, whereas studies with solid IR on KBr disks were performed using a Mattson Sirius Research FTIR spectrometer. Electrospray mass spectrometry was carried out on a Finnigan LCQ, and electron ionization was done using a Fission Instruments Autospec mass spectrometer. Silica column chromatography was carried out using silica gel provided by Fluorochem Ltd. (35–70  $\mu\text{m}$ ). Thin-layer chromatography was performed on commercially available Merck aluminum-backed silica plates. Preparative gel permeation chromatography was carried out using a 2 m glass column packed with Biobeads SX-1, supplied by Biorad. Analytical gel permeation chromatographs were recorded using a Waters instrument incorporating two Shodex columns in series (KF-802.5 and KF-803) using THF as eluent. The electrochemical studies were carried out on an EG & G Princeton Applied Research potentiostat/galvanostat model 273 with a standard three-electrode configuration, consisting of platinum working (0.5 mm diameter disk) and counter electrodes and an Ag/AgCl reference electrode. Each compound was studied in a supporting electrolyte of (typically) 0.2 M  $[\text{Bu}_4\text{N}]^+[\text{BF}_4]^-$  using scan rates of 50–500  $\text{mV s}^{-1}$ .

**Solvent Preparation.** THF was refluxed over Na and benzophenone for a minimum of 24 h before being collected by distillation. Dichloromethane was similarly dried over calcium hydride, and dry MeOH was obtained by refluxing over calcium sulfate for 1–2 h, prior to collection by distillation. Other reagents and solvents were used as received. Dendritic branches **6**, **7**, and **8** were prepared according to minor modifications of literature procedures.<sup>15</sup>

**Synthesis of 1,1'-Bis(*tert*-butyl)aminocarbonylferrocene [**G0(Fc)**].** 1,1'-Bis(fluorocarbonyl)ferrocene (75 mg, 0.27 mmol) was dissolved in dry  $\text{CH}_2\text{Cl}_2$  (2 mL) under an atmosphere of  $\text{N}_2$ . To it was added *tert*-butylamine (40 mg, 0.54 mmol) in dry  $\text{CH}_2\text{Cl}_2$  (2 mL), followed by DMAP (67 mg, 0.54 mmol). The reaction mixture was allowed to stir at ambient temperature for 24 h and was followed by TLC (silica,  $\text{CH}_2\text{Cl}_2$ –MeOH 90:10). The solvent was evaporated from the reaction mixture, and the products were separated by column chromatography (silica,  $\text{CH}_2\text{Cl}_2$ –MeOH 90:10), to obtain the desired product (77 mg, 74% yield).

Yellow solid.  $R_f = 0.59$  ( $\text{CH}_2\text{Cl}_2$ –MeOH 90:10).  $^1\text{H}$  NMR (270 MHz,  $\text{CDCl}_3$ ):  $\delta$  6.37 (2H, bs, NH), 4.42 (4H, app s, Fc–H), 4.32 (4H, app s, Fc–H), 1.46 (18H, s,  $\text{CH}_3$ ).  $^{13}\text{C}$  NMR (68.75 MHz,  $\text{CDCl}_3$ ):  $\delta$  169.4 (C=O), 79.4 (FcC–C), 70.8 (FcC–H), 70.6 (FcC–



H), 51.5 ( $C(CH_3)_3$ ), 28.9 ( $CH_3$ ). IR (KBr disk):  $\nu_{max}$  3325m (NH), 3088w, 2963w, 1634s ( $C=O$ ), 1539s, 1446m, 1363w, 1309m, 1221m, 1022w, 822w. MS (electrospray):  $m/z$  (relative intensity)  $[M + Na]^+$  requires 407, found 407 (100), 408 (20), 385 ( $[M + H]^+$ , 21). HRMS (FAB) ( $C_{20}H_{28}N_2O_2Fe$ ): found 384.1505, calculated 384.1500.

**Synthesis of G1(Fc).** 1,1'-Bis(chlorocarbonyl)ferrocene (0.25 g, 0.8 mmol) was dissolved in dry  $CH_2Cl_2$  (5 mL) under  $N_2$ . To it were added first generation dendritic branch (**6**)<sup>15</sup> (0.91 g, 2.4 mmol) and DMAP (0.29 g, 2.4 mmol). The mixture was then stirred in the dark, under  $N_2$  at room temperature for 24 h. The mixture was filtered and separated on a gel column (Biobeads, SX-1) to obtain the pure product as the fastest eluting orange band (413 mg, 51% yield).

Orange oil.  $R_f = 0.62$  ( $CH_2Cl_2$ -MeOH 90:10).  $^1H$  NMR ( $CDCl_3$ , 270 MHz):  $\delta$  4.66 (4H, s, Fc-H), 4.31 (4H, s, Fc-H), 3.65 (42H, m,  $CO_2CH_3$ ,  $OCH_2CH_2$ ,  $CH_2OCH_2$ ), 2.56 (12H, t,  $J = 6.0$  Hz,  $OCH_2CH_2$ ).  $^{13}C$  NMR ( $CDCl_3$ , 68.75 MHz):  $\delta$  [peaks associated with the ferrocene core were low intensity] 171.9 ( $CO_2CH_3$ ), 169.8 (CONH), 78.0 (Fc-C), 72.3 (Fc-H), 70.9 (Fc-H), 69.1 ( $CH_2OCH_2$ ), 66.7 ( $CH_2OCH_2$ ), 59.9 (C-NH), 51.6 ( $CO_2CH_3$ ), 34.7 ( $CH_2COOMe$ ). IR (neat):  $\nu_{max}$  3398w and 3323w (NH), 2953m and 2878m (CH), 1739s (CO ester), 1654m (CO amide), 1521m, 1439m, 1367m, 1268m, 1171m, 1113m (CO amide), 1075m (CO ether), 1025m. MS (electrospray):  $m/z$  (relative intensity)  $[M + Na]^+$  requires 1019, found 1019 (100), 1020 (44). HRMS (FAB) ( $C_{49}H_{64}N_2O_{20}FeNa$ ): found 1019.3307, calculated 1019.3300.

**Synthesis of G2(Fc).** To 1,1'-bis(chlorocarbonyl)ferrocene (41 mg, 0.13 mmol) were added the second generation dendritic branch (**7**)<sup>15</sup> (408 mg, 0.29 mmol) in dry  $CH_2Cl_2$  (10 mL) with stirring at room temperature and DMAP (16 mg, 0.13 mmol). The mixture was stirred in the dark, under  $N_2$  for 4 days. The product mixture was then separated by gel permeation chromatography (Biobeads, SX-1, eluting with  $CH_2Cl_2$ ), and the first colored band was collected and rotary evaporated to give the highest mass product, i.e., bis-substituted dendritic product **G2(Fc)** (137 mg, 34%).

Orange oil.  $R_f = 0.55$  ( $CH_2Cl_2$ -MeOH 90:10). Analytical GPC,  $t_R = 17.89$  (THF, 1 mL  $min^{-1}$ ), corresponding to  $M_r$  2606 after performing calibration with linear polystyrene.  $^1H$  NMR ( $CDCl_3$ , 500 MHz):  $\delta$  6.14 (8H, br m, N-H), 4.75 (4H, br s, Fc-H), 4.32 (4H, br s, Fc-H), 3.65 (150H, m,  $CH_2OCH_2CH_2CO_2CH_3$ ,  $CH_2OCH_2CH_2CONH$ ), 2.52 (36H, br app s,  $OCH_2CH_2CO_2Me$ ), 2.43 (12H, br app s,  $OCH_2CH_2$ -

CONH).  $^{13}C$  NMR ( $CDCl_3$ , 125 MHz):  $\delta$  [the ferrocene core was not observed in the  $^{13}C$  NMR] 171.9 ( $CO_2CH_3$ ), 171.3 (CONH), 69.6 ( $CH_2OCH_2$ ), 68.1 ( $CH_2OCH_2$ ), 67.2 ( $CH_2OCH_2$ ), 60.4 (C-NH), 60.2 (C-NH), 52.1 ( $CO_2CH_3$ ), 37.7 ( $CH_2CONH$ ), 35.2 ( $CH_2COOMe$ ). IR (neat):  $\nu_{max}$  3380w (NH), 2928m and 2874m (CH), 1738s (CO ester), 1650m (CO amide), 1438m, 1366m, 1266m, 1179s, 1112s, 737m. MS (electrospray):  $m/z$  (relative intensity) observed  $[M + 2Na]^{2+}$  ( $M_r = 3124$ , doubly charged ion therefore will appear at 1562) 1563.2 (60), 1563.7 (52); also observed  $[M + Na + K]^{2+}$  ( $M_r = 3141$ , doubly charged ion therefore will appear at 1570.5) 1569.7 (40), 1571.2 (35), 1571.7 (25); also observed singly charged ion corresponding to the fragment  $[CpCONH(G2\text{-branch})]^+$  1535.7 (100), 1536.7 (80); other unassigned fragments 1443.7 (40), 1421.5 (20), 1326.5 (20)—note all these fragments are artifacts of the MS process as GPC clearly indicated a single high-mass product ( $M_r > 2500$ ).

**Synthesis of G1(Fc-ether).** The first generation branch substituted with oligoether groups at the periphery (**8**)<sup>15</sup> (144 mg, 0.19 mmol) was dissolved in dry THF (5 mL), and to it were added 1,1'-bis(chlorocarbonyl)ferrocene (21 mg, 0.07 mmol) and DMAP (23 mg, 0.19 mmol). The reaction was stirred, under  $N_2$ , in the dark at room temperature for 7 days. The products were then separated by preparative GPC (Biobeads, SX-1,  $CH_2Cl_2$ ) to give the desired product (91 mg, 73%).

Orange oil.  $^1H$  NMR ( $CDCl_3$ , 270 MHz):  $\delta$  6.27 (8H, br s, N-H), 4.67 (4H, br s, Fc-H), 4.30 (4H, br s, Fc-H), 4.21 (12H, br s,  $COOCH_2$ ), 3.75–3.52 (84H, m,  $CH_2OCH_2$ ), 3.35 (18H, s,  $OCH_3$ ), 2.56 (12H, br t,  $CH_2COOR$ ). IR (neat):  $\nu_{max}$  3510w, 3421w (NH), 2878m (CH), 1732s (CO ester), 1644w, 1522w, 1455w, 1257w, 1186m, 1107s, 1037m, 851w. MS (electrospray):  $m/z$  (relative intensity)  $[M + Na]^+$  requires 1811, found 1811.8 (100), 1812.8 (77), 1813.8 (45), 1789.5 ( $[M + H]^+$ , 95), 1790.5 (70), 1791.5 (45).

**Acknowledgment.** D.K.S. acknowledges EPSRC and Cytec-fiberite for the award of a CASE studentship (to D.L.S.), Professor Paul Walton for the use of electrochemistry equipment, Graham Dykes for running high resolution NMR spectra, and The University of York for other financial support.

JA0117478